PHYSICAL REVIEW E **73**, 045603(R) (2006)

Nontopological Raman-Kerr self-induced transparency solitons in photonic crystal fibers

D. V. Skryabin,* A. V. Yulin, and F. Biancalana†
Centre for Photonics and Photonic Materials, Department of Physics, University of Bath, Bath BA2 7AY, United Kingdom
(Received 9 December 2005; published 17 April 2006)

Using analytical and numerical methods we demonstrate that the pulse propagation equations accounting for the quantum description of the Raman transition and for the optical Kerr nonlinearity have a multiparameter family of nontopological solitary wave solutions. We study properties of these solitons and report the transition from stable to unstable regimes of propagation. We also discuss the feasibility of observation of these structures in gas filled hollow-core photonic crystal fibers.

DOI: 10.1103/PhysRevE.73.045603 PACS number(s): 42.65.Tg, 42.50.Gy, 42.65.Dr, 42.50.Md

Interaction of short optical pulses with resonant transitions in atomic or molecular media has attracted significant research efforts from the 1960s up to the present day. Self-induced transparency (SIT) of optical pulses in the two-level model, see, e.g., Ref. [1], and soliton effects in electromagnetically induced transparency (EIT), see, e.g., Ref. [2], are the most prominent soliton related results in this research area. The relatively recent invention of hollow-core photonic crystal fibers [3] (HC-PCFs) has created favorable conditions for renewing experimental efforts along these lines. Indeed, long propagation distances, low losses, and tight focusing with simultaneous complete suppression of diffraction make HC-PCFs filled with gases or liquids at least worth trying, and at most an ideal environment for experiments on resonant nonlinear and quantum optics in general and on soliton propagation especially.

Very recent experiments done in the cw and in the quasi-cw regimes have demonstrated a dramatic increase in the efficiency of the stimulated Raman scattering in gas-filled HC-PCFs [4], and EIT in acetylene filled HC-PCFs [5]. The use of femtosecond pump sources for similar experiments is likely to happen soon. Propagation of short pulses in HC-PCFs poses, however, several theoretical problems, which previously have not been relevant. Among those, are the roles played by the fiber dispersion [6] and by the intrinsic Kerr nonlinearity of the HC-PCF [7]. In this work, we consider solitons in the HC-PCF filed with a Raman active gas. The main difference with our recent work [8] and with many other papers on Raman solitons, see, e.g., Ref. [9], is that here we assume a strong excitation, so that the both levels participating in the Raman transition can be populated, and not just the ground state. This assumption does not just add new features into the system, but introduces a family of gap solitons not related to the nonlinear-Schrödinger (NLS) type solitons reported for far off-resonance Raman transition [8,10]. Combined SIT-NLS solitons, related to the Raman solitons studied below, have been previously reported, e.g., in Ref. [11].

We assume that the two optical pulses with envelopes described by the functions $B_{1,2}(z,t)$ and with carrier frequencies $\omega_1 > \omega_2$ are coupled by a Raman transition with frequency $\omega_R = \omega_1 - \omega_2$ and by the Kerr nonlinearity. For the sake of simplicity, we assume that the higher-order Stokes and anti-Stokes components are suppressed due to high losses [4]. The corresponding dimensionless equations are

$$i[\partial_z + s\partial_t]B_1 = -QB_2 - \tilde{\gamma}[|B_1|^2 + 2|B_2|^2]B_1, \tag{1}$$

$$i[\partial_z - s\partial_t]B_2 = -Q^*B_1 - \tilde{\gamma}[|B_2|^2 + 2|B_1|^2]B_2, \tag{2}$$

$$i\left[\partial_t + \frac{\tau_0}{T_2}\right]Q = -B_1B_2^*\sigma, \tag{3}$$

$$\partial_t\sigma + \frac{\tau_0}{T_1}[\sigma - 1] = -\frac{i}{2}[B_1B_2^*Q^* - B_1^*B_2Q]. \tag{4}$$

Here Q is the Raman coherence and σ is the population inversion of the two levels separated by $\hbar\omega_R$. $\sigma=1$ corresponds to the ground state of the Raman transition. $\tilde{\gamma}$ characterizes the Kerr nonlinearity of the HC-PCF [7]. $T_{1,2}$ are the decay times of σ and Q. For an ideal soliton solution to exist one should assume that $\tau_0/T_{1,2} \to 0$. The derivation of Eqs. (1) and (2), with $\tilde{\gamma}=0$, from the first principles can be found for example in Ref. [1]. Parameter s characterizes the difference in the group velocities of the two waves and it can be normalized to any convenient number. Without loss of generality we fix $s=-1$. Detailed discussion of the normalization procedure in the context of the HC-PCFs is given at the end of the paper.

The condition that the total population of the two levels is 1, can be expressed as

$$\sigma^2 + |Q|^2 = 1. \tag{5}$$

Equation (5) suggests the well known substitution

$$\sigma = \pm\cos\phi, \quad Q = e^{i\alpha}\sin\phi, \tag{6}$$

which allows the derivation of a pendulum like equation for ϕ [12]. The constant phase α and the $\pm$ sign can be fixed as convenient. For $\tilde{\gamma}=0$, this approach leads to explicit soliton solutions with exponential (π soliton) or algebraic (2π soliton) tail decay, as first reported in Ref. [12]. In our notations, the π solitons are given by

*Author to whom correspondence should be addressed. Email address: d.v.skryabin@bath.ac.uk; URL: http://staff.bath.ac.uk/pysdvs
†Present address: Tyndall National Institute, Lee Maltings, Cork, Ireland.

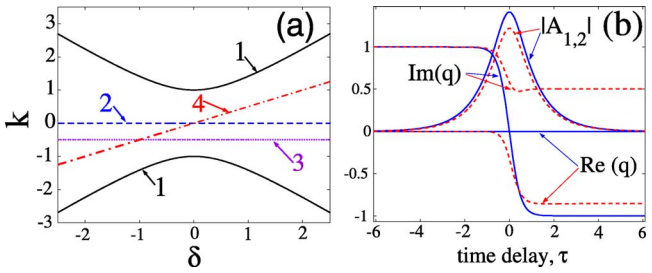

FIG. 1. (Color online) (a) Dispersion characteristics of the linear waves for $|q_\infty|=1$ are shown by the full black lines marked with 1. Straight lines indicate spectral content of the soliton. Line 2 corresponds to $\kappa=v=0$. Line 3 corresponds to $v=0$, $\kappa=0.5$. Line 4 corresponds to $\kappa=0$, $v=0.5$. (b) τ dependence of ReQ, ImQ, and $|A_{1,2}|$ for the soliton solutions at $\kappa=v=0$. Full lines correspond to the topological soliton at $\tilde{\gamma}=0$ and the dashed lines correspond to the nontopological one at $\tilde{\gamma}=0.3$.

$$B_1 = i\sqrt{\frac{2\,\mathrm{sech}(2\tau w)}{1+v}}, \quad B_2 = \sqrt{\frac{2\,\mathrm{sech}(2\tau w)}{1-v}},$$

$$Q = \tanh(2\tau w), \quad \sigma = -\,\mathrm{sech}(2\tau w), \quad w = 1/\sqrt{1-v^2}, \quad (7)$$

where $\tau=t-vz$ and v is the parameter associated with the shift of the common group velocity. By analogy with the model of the two-level atom, these solitons can be called Raman-SIT solitons.

Below we will demonstrate that the above solution represents a particular subset of a more general family of soliton solutions, which can be either dynamically stable or unstable. As one can see, the Raman coherence Q in the above solution has the topological structure of a dark soliton, so that its amplitude is zero and the phase has a discontinuity at the center. It will be demonstrated below that the topological structure is not actually necessary for the soliton existence and most typically the phase of Q varies smoothly across the soliton.

The first step in our analysis is to understand the dispersive properties of the linear waves. Substituting $B_{1,2}\sim e^{-ikz-i\delta t}$ into Eqs. (1) and (2), assuming some stationary value of the Raman coherence Q and neglecting nonlinearity we find that $k=\pm\sqrt{\delta^2+|Q|^2}$. Therefore, nonzero Q opens up the gap in the wave numbers forbidden for propagation of linear waves, see Fig. 1(a). Propagation of the solitons with spectrum residing within this gap can, however, be allowed. For other examples of the solitons supported by the wave number band gaps see, e.g., Ref. [13]. The existence of two independent and arbitrary phase rotations $(A_1,A_2,Q)\to(A_1e^{i\alpha_1+i\alpha_2},A_2e^{i\alpha_1-i\alpha_2},Qe^{2i\alpha_2})$ suggests that we should seek soliton solutions in the form

$$B_{1,2} = A_{1,2}(\tau)e^{-i\kappa z\mp i\beta z-i\beta t}, \quad Q = q(\tau)e^{-i2\beta z}, \quad \tau = t-vz. \quad (8)$$

$A_{1,2}$ obeys the ordinary differential equations

$$[\kappa - i(1+v)\partial_\tau]A_1 = -qA_2 - \tilde{\gamma}[|A_1|^2+2|A_2|^2]A_1,$$

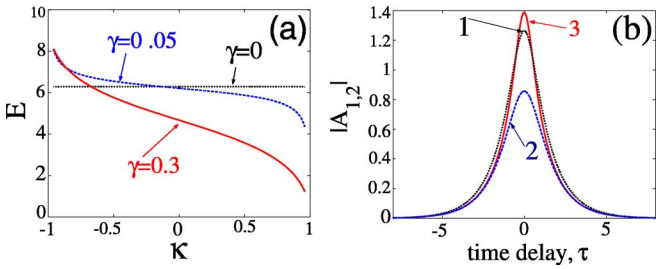

FIG. 2. (Color online) (a) The total field energy E vs κ for different values of $\tilde{\gamma}$ and $v=0$. (b) $|A_{1,2}|$ vs τ for $v=0$. Line 1 corresponds to $\tilde{\gamma}=0$ and $\kappa=\pm0.7$. Line 2 corresponds to $\tilde{\gamma}=0.3$ and $\kappa=0.7$. Line 3 corresponds to $\tilde{\gamma}=0.3$ and $\kappa=-0.7$. The full pulse width at the half maximum is $\simeq3$ for 2 and $\simeq2$ for 3.

$$[\kappa + i(1-v)\partial_\tau]A_2 = -q^*A_1 - \tilde{\gamma}[|A_2|^2+2|A_1|^2]A_2. \quad (9)$$

Here κ and v parameterize the soliton family and their role is detailed below. β affects the phases of the two fields and Raman coherence, but not their amplitudes. For the soliton spectrum to remain within the band gap, the parameters must obey the inequality $\kappa^2<|q_\infty|^2(1-v^2)$, where $|q_\infty|$ is the coherence amplitude far from the soliton core, see Fig. 1(b).

We solved the nonlinear system of ordinary differential equations for $A_{1,2}$, q, and σ numerically, using Eq. (5) as one of the boundary conditions. We focus here on the case $|q_\infty|=1$ and $\sigma_\infty=0$, i.e., the medium is prepared with coherence and equal population of both levels. See, e.g., Ref. [14] for methods of such preparation. Another interesting case is $q_\infty=0$ and $\sigma_\infty=1$, i.e., where the medium is unprepared and the upper level is not populated. In this case the band gap is closed and therefore the exponential decay of tails is replaced by the algebraic one. Though most of our results below can be extended to the case of the algebraic solitons, we prefer to focus here on the more practical and robust case of the exponentially localized ones. Figure 1(b) shows the time profiles of the Raman coherence and of $|A_1|=|A_2|$ for $\kappa=v=0$, $\tilde{\gamma}=0$ (full lines), and $\tilde{\gamma}=0.3$ (dashed lines). One can clearly see the change of the topological($\tilde{\gamma}=0$) to the nontopological ($\tilde{\gamma}\neq0$) structure of Q.

The parameter κ controls the nonlinearity related shift of the soliton wave number within the band gap. When $\kappa>0$, the soliton spectrum is shifted towards the lower boundary of the bandgap where $\partial^2k/\partial\delta^2<0$, see Fig. 1(a). This corresponds to the effective anomalous group velocity dispersion (GVD), which in the presence of the self-focusing Kerr nonlinearity ($\tilde{\gamma}>0$) triggers the soliton formation mechanisms known for the NLS equation. NLS-type solitons become wider and less energetic, when their spectrum is reaching the spectrum of the anomalously dispersing linear waves. Therefore, the soliton energy

$$E = \int (|A_1|^2+|A_2|^2)d\tau = E_1+E_2, \quad (10)$$

is expected to decrease for κ increasing, see Fig. 2. If $\tilde{\gamma}=0$, then E does not depend on κ. In this case the dependence of the soliton solutions on κ can be found analytically. First, we

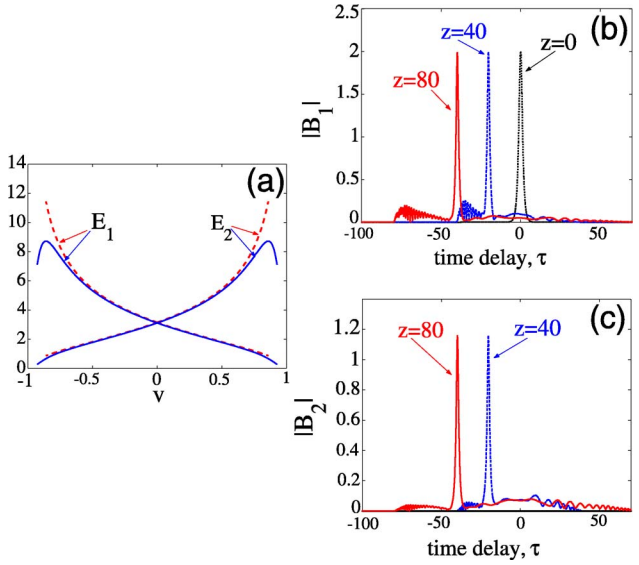

FIG. 3. (Color online) (a) Energies of the soliton components $E_{1,2}$ vs v for $\kappa=0$. The dashed lines are for $\tilde{\gamma}=0$ and the full ones are for $\tilde{\gamma}=0.05$. (b), (c) Formation of the Raman SIT soliton from the initial conditions $B_1=2\,\mathrm{sech}(t)$, $B_2=0$.

observe that the identity (5) can be satisfied by a more general substitution, than Eq. (6), namely

$$q = e^{i\alpha}[i\sin\psi + \cos\psi\sin\phi], \quad \sigma = \pm\cos\psi\cos\phi, \tag{11}$$

where ψ and ϕ are the two angles to be determined. With some algebra we have demonstrated that Eqs. (3), (4), (8), and (9) for $v=\tilde{\gamma}=0$ are satisfied providing that $\sin\psi=-\kappa$, $\tan(\phi/2)=-\tanh(t\sqrt{1-\kappa^2})$ and $\kappa\in(-1,1)$. This gives the soliton solutions in the form

$$B_1 = i\sqrt{2h\,\mathrm{sech}(2th)}e^{-i\kappa z-i\beta z-i\beta t},$$

$$B_2 = \sqrt{2h\,\mathrm{sech}(2th)}e^{-i\kappa z+i\beta z-i\beta t}, \quad h=\sqrt{1-\kappa^2}$$

$$Q = h\tanh(2th) - i\kappa, \quad \sigma = -h\,\mathrm{sech}(2th). \tag{12}$$

One can see that for $\kappa\neq 0$, Q is a complex function with no phase discontinuity at the soliton center, and so the topological structure is destroyed already for $\tilde{\gamma}=0$. The energy of the solution (12) does not depend on κ, because the h parameter can be scaled away from the integral (10).

Parameter v controls the slope of the line representing the soliton spectrum within the band gap, see Fig. 1(a), and hence, the relative energies of the two optical fields. Indeed, when v is deviated from zero to the positive (negative) side then the soliton spectrum starts approaching the line $k=-\delta$ ($k=\delta$), which is the dispersion characteristic of the field B_2 (B_1) for $Q=0$. The balance of power between the soliton components changes accordingly [see Fig. 3(a)]. Excitation of a two-frequency Raman SIT soliton by a single frequency pump pulse is demonstrated in Figs. 3(b) and 3(c).

We restricted stability analysis of the Raman-Kerr solitons to direct numerical simulations of Eqs. (1)–(4) initialized with the solitons. Our numerical scheme was based on the

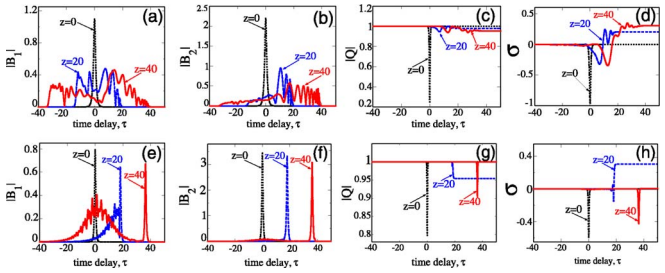

FIG. 4. (Color online) Different scenario of the soliton instability for $\tilde{\gamma}=0.05$. (a)–(d) are for $v=0.6$, $\kappa=0$, and (e) and (h) are for $v=0.9$, $\kappa=0$. (a) and (e) show $|B_1|$, (b) and (f) show $|B_2|$, (c) and (g) show $|Q|$, (d) and (h) show σ.

method of alternating directions. Integration of the equations for Q and σ in t has been done using the five point implicit Adams method. Integration of the equations for $B_{1,2}$ in z was done using splitting of a single z step into three successive steps with the exact analytical solutions found for $B_{1,2}$ at each of them. An extensive series of simulations unambiguously indicate that the topological solitons are stable, while the finite values of the Kerr nonlinearities and/or κ lead to destabilization of the solitons in some parts of the parameter space, but not in the entire range of the soliton existence. Physically, we relate the instability to the unbalanced competition between the SIT-like soliton supporting mechanism on one side and effective GVD felt by the solitons and the focusing Kerr nonlinearity on the other.

Let us now fix $\tilde{\gamma}=0.05$ and discuss soliton evolution for $\kappa=0$ and various values of v. For v exactly equal or close to zero the initial soliton profile is weakly unstable. It undergoes adiabatic change in its velocity, but nevertheless retains its localized shape over the propagation distance order of 100 dimensionless units. With v increasing, the unstable behavior becomes more and more noticeable. For example for $v=0.6$, see Figs. 4(a)–4(d), the soliton is quickly destroyed by the perturbations. The character of the instability changes, however once v starts approaching 1, see Figs. 4(e)–4(h). Now the instability shows itself through the emission of the nonlocalized dispersive radiation most noticeable in the weaker soliton component, see Figs. 4(e) and 4(f), where $v=0.9$ initially. After the emission process is over, a stable solitonic structure is formed, which propagates with a slightly different velocity and a noticeably different value of κ. The value of κ changes from the initial $\kappa=0$ to $\kappa\simeq 0.11$. The positive values of κ increase anomalous GVD [see Fig. 1(a) and the arguments before Eq. (10)]. This restores the balance between the effective GVD and Kerr nonlinearity, thereby suppressing the instability. The soliton solution found from Eqs. (9) and (10) for $\kappa=0.11$, $v=0.91$, and $\tilde{\gamma}=0.05$ appears to be stable in our modeling. Deviating κ towards the negative side, i.e., $\kappa<0$, shifts the soliton spectrum towards the upper branch of the linear waves having normal GVD, $\partial^2 k/\partial\delta^2>0$, and therefore enhances the instability.

Attempts to observe Raman SIT solitons in experiments are likely to face the following difficulty: The dispersion of unconfined gas or gas in a cell is relatively low. Therefore, the group velocity mismatch between the two fields is naturally small, which implies that the two branches of

the dispersion characteristics, in Fig. 1(a), are close to be parallel and the GVD induced by the Raman coherence is small. This in its turn means narrow and hence intense solitons. Therefore, in order to reduce the peak powers one should look for means of increasing the difference in the group velocities of the two fields. HC-PCFs are strongly dispersive [6] and therefore are expected to provide significant reduction of the power requirements relative to gas cells or weakly guiding capillaries. If $\beta(\omega)$ is the propagation constant of a relevant fiber mode then $\beta_{1,2}^{(1)}=\partial_\omega\beta(\omega_{1,2})$ are the group velocities at the two frequencies of interest and $s=\mathrm{sgn}(\beta_1^{(1)}-\beta_2^{(1)})$. Dimensionless coordinate z and time t are linked with the physical distance Z and physical time T as $t\tau_0=T-Z[\beta_1^{(1)}+\beta_2^{(1)}]/2$, $Z=z_0z$. Convenient choices for z_0 and τ_0 are $z_0=2\tau_0/|\beta_1^{(1)}-\beta_2^{(1)}|$ and $\tau_0=\sqrt{2T_2/[g_{ss}\hbar\omega_1N_0]}|\beta_1^{(1)}-\beta_2^{(1)}|$, so that z_0 is the characteristic walk-off length. Here N_0 is the density of molecules and g_{ss} is the steady-state Raman gain [1]. Note that we have neglected in this work the intrinsic GVD of the fiber itself, by making a realistic assumption that $\omega_{1,2}$ and pulse duration are such that the corresponding GVD lengths are much longer than z_0. Using data for the typical PCF design, see, e.g., Refs. [7,8], we can estimate $|\beta_1^{(1)}-\beta_2^{(1)}|\simeq 0.02/c$, where c is the speed of light in vacuum. $\tilde{\gamma}$ characterizes the relative strength of the Kerr and Raman nonlinearities: $\tilde{\gamma}=[2\gamma S/|\beta_1^{(1)}-\beta_2^{(1)}|]\sqrt{\hbar\omega_1T_2N_0/g_{ss}}$, where S is the effective area of the fiber mode and γ is the intrinsic Kerr nonlinearity of the fiber. A unit amplitude of $|B_{1,2}|^2$ corresponds to the peak power $\tilde{\gamma}/[z_0\gamma]\sim|\beta_1^{(1)}-\beta_2^{(1)}|^{-1}$, which agrees with our qualitative arguments. Choosing SF_6 gas as an example we have $g_{ss}\sim 14\times10^{-14}$ m/W, and $\omega_R\simeq 2\pi\times 23$ THz. T_2 depends on pressure and on collisions with the glass walls. For our estimates we use $T_2\simeq 5$ ps, see, e.g., Ref. [15]. This gives $z_0\simeq 8$ mm and $\tau_0\simeq 200$ fs. Taking $S\simeq 60$ μm^2 and γ from $10^{-6}1/(\mathrm{W\,m})$ to $10^{-5}1/(\mathrm{W\,m})$, gives us $\tilde{\gamma}\sim 0.02$–0.2 and typical scaling for the peak power ~ 2 MW. Thus the estimates for the typical pulse durations and peak powers are realistic [7] and can be further optimized through the fiber design, choice of gas and conditions of operation.

This work has been supported by the Leverhulme Trust.

[1] A. I. Maimistov and M. Basharov, *Nonlinear Optical Waves* (Kluwer Academic Publishers, 1999); A. C. Newell and J. V. Moloney, *Nonlinear Optics* (Addison-Wesley, Redwood City, 1992).

[2] R. Grobe, F. T. Hioe, and J. H. Eberly, Phys. Rev. Lett. **73**, 3183 (1994); A. Kasapi, M. Jain, G. Y. Yin, and S. E. Harris, *ibid.* **74**, 2447 (1995); J. Cheng, S. Han, and Y. J. Yan, Opt. Lett. **30**, 2638 (2005).

[3] P. St. J. Russell, Science **299**, 358-362 (2003).

[4] F. Benabid, J. G. Bouwmans, J. C. Knight, P. S. J. Russell, and F. Couny, Phys. Rev. Lett. **93**, 123903 (2004).

[5] S. Ghosh, J. E. Sharping, D. G. Ouzounov, and A. L. Goeta, Phys. Rev. Lett. **94**, 093902 (2005).

[6] C. M. Smith *et al.*, Nature (London) **424**, 657 (2003).

[7] D. G. Ouzounov *et al.*, Science **301**, 1702 (2003); F. Luan *et al.*, Opt. Express **12**, 835 (2004).

[8] D. V. Skryabin, F. Biancalana, D. M. Bird, and F. Benabid, Phys. Rev. Lett. **93**, 143907 (2004).

[9] F. Y. F. Chu and A. C. Scott, Phys. Rev. A **12**, 2060 (1975); G. S. McDonald, Opt. Lett. **20**, 822 (1995); M. Scalora, S. Singh, and C. M. Bowden, Phys. Rev. Lett. **70**, 1248 (1993).

[10] D. D. Yavuz, D. R. Walker, and M. Y. Shverdin, Phys. Rev. A **67**, 041803(R) (2003).

[11] A. I. Maimistov and E. A. Manykin, Zh. Eksp. Teor. Fiz. **85**, 1177 (1983) [Sov. Phys. JETP **58**, 685 (1983)]; M. Nakazawa, E. Yamada, and H. Kubota, Phys. Rev. Lett. **66**, 2625 (1991).

[12] T. M. Makhviladze and M. E. Sarychev, Sov. Phys. JETP **44**, 471 (1977); A. E. Kaplan, Phys. Rev. Lett. **73**, 1243 (1994).

[13] C. M. de Sterke and J. E. Sipe, Phys. Rev. A **42**, 550 (1990); G. Van Simaey, S. Coen, M. Haelterman, and S. Trillo, Phys. Rev. Lett. **92**, 223902 (2004); D. V. Skryabin, Opt. Express **12**, 4841 (2004).

[14] J. R. Kuklinski, U. Gaubatz, F. T. Hioe, and K. Bergmann, Phys. Rev. A **40**, R6741 (1989).

[15] M. Wittmann, A. Nazarkin, and G. Korn, Phys. Rev. Lett. **84**, 5508 (2000).